The Kalman filter uncertainty concept in the possibility domain

A. Ferrero[1], $Fellow, IEEE$, R. Ferrero[2], $SeniorMember, IEEE$,
W. Jiang[3], S. Salicone[1], $SeniorMember, IEEE$,

***Abstract*—The Kalman filter is one of the most important and common optimal recursive data processing algorithm in many applications characterized by linear dynamical behavior and affected by random zero-mean white Gaussian noise. However, when measurement processes are considered, inaccuracy is not only due to noise, but also to several contributions to uncertainty that can be due to both random and uncompensated systematic effects. Therefore, when the Kalman filter is used on experimental data, all uncertainty contributions should be considered.**

While several proposals are available in the literature to modify the Kalman filter in order to consider different probability distributions and systematic effects, represented both in probability and possibility domains, they are not fully compliant with the uncertainty concept adopted in metrology. The aim of this paper is hence to reformulate the Kalman filter theory within the possibility domain in compliance with the measurement uncertainty concept, in order to be able to consider both the random and systematic contributions to uncertainty (regardless of their distribution) that may affect the measurement process.

An experimental set-up is considered and the results obtained under different assumptions are reported.

***Index Terms*—Measurement Uncertainty; Possibility distributions; Random-Fuzzy Variables; Random contributions; Systematic contributions.**

I. Introduction

The Kalman filter (KF) [1] is a widely-employed algorithm in system state identification that improves the accuracy in state identification by combining the available information about the uncertainties associated to the system model and those associated to the measured values.

According to the classical Kalman filter theory, uncertainties affecting the system and the measured values are represented by random contributions with normal, zero-mean probability distribution (PDF). Modeling uncertainty as noise with normal, zero-mean PDF has represented a limitation of the classical Kalman filter, when employed in measurement applications, under several points of view.

The main point is that noise is only one of the several uncertainty contributions affecting a measurement procedure and several contributions exist that cannot be correctly represented with a normal, zero-mean PDF. For instance, one of the most important uncertainty contributions, in digital instruments, is the quantization error, which is generally modeled as a quantization noise with uniform PDF inside the quantization band. In order to consider different PDFs than the normal one, the unscented Kalman filter (UKF) has been proposed [2] and efficiently applied in measurement applications [3].

Moreover, random effects are not the only contributions to uncertainty. Despite the Guide to the expression of Uncertainty in Measurement (GUM) [4] recommends to identify all possible systematic effects and apply suitable compensations for, situations may occur where a complete identification is not possible and compensation is either unpractical or too expensive. Therefore, systematic effects must be taken into account too. Modifications of the classical Kalman filter have been proposed [5]–[8] to consider also systematic effects.

Recent studies have challenged the effectiveness of probability in representing, evaluating and combining the uncertainty contributions due to systematic effects, especially when only limited information is available about those contributions, as largely proved, on the basis of several practical examples, by [9]–[11]. The recent mathematical theory of possibility [12], [13] has been proposed as a more efficient mathematical tool to handle uncertainty under such conditions in a GUM [4] compliant way [14]–[18].

Given the importance of the Kalman filter in several measurement applications, it is interesting to investigate how it can be extended from the probabilistic to the possibilistic domain. Several methods and applications have been already proposed [19], [20] and proved that possibility distributions (PDs) can be effectively employed, instead of PDFs, to model the noise terms of the classical Kalman filter.

At the Authors' knowledge, the available possibilistic techniques applied in Kalman filters model uncertainty in a kind of semantic way, as typical of the fuzzy applications. On the other hand, when measurement applications are considered, uncertainty is a very specific concept with a definite meaning, as recommended by the GUM [4] in accordance with the definition given by the International Vocabulary of Metrology (VIM) [21]. It is therefore important that, whenever measurement uncertainty is considered, it is modeled and represented in such a way that compliance with those official documents is assured, at least in the concepts.

Compliance with the GUM-defined measurement uncertainty concept is granted by the recent proposal to represent a measurement result, together with the appertaining uncertainty, with a Random-Fuzzy variable (RFV) within the possibility theory [17], [18], [22], which was succesfully applied in sev-

The authors are with: [1]Department of Electronics, Information and Bioengineering, Politecnico di Milano, p.za Leonardo da Vinci 32, I-20133 Milano, Italy (e-mail: alessandro.ferrero@polimi.it, simona.salicone@polimi.it); [2]Department of Electrical Engineering and Electronics, University of Liverpool, Liverpool L69 3GJ, UK (e-mail: roberto.ferrero@liverpool.ac.uk); [3] College of Mechatronics Engineering and Automation, National University of Defense Technology, Changsha - 410073 - China (e-mail: jiangweinudt@gmail.com)

eral different fields [23]–[26]. This approach leads to represent and propagate the effects (on the considered measurement result) of both the random and systematic uncertainty contributions. This generalization appears then to be particularly suitable to ensure GUM compliance also to Kalman filter applications in the instrumentation and measurement domain, when all kinds of possible contributions to uncertainty are considered and represented with RFVs. It is hence worth, as initially shown in [27], to reformulate the Kalman filter theory in terms of RFVs, so that different kinds of random and systematic contributions to uncertainty can be considered in a GUM compliant way [18].

This paper starts from the theoretical formulation given in [27] (and here extensively recalled for the sake of clarity), reviews it and shows a practical experimental example. The results obtained under different metrological assumptions are shown.

The paper is organized as follows: Section II briefly recalls the classical Kalman filter. Section III recalls some basic definitions of the Random-Fuzzy variables and exploits them to implement a possibilistic Kalman filter as a direct extension of the classical one. Section IV proposes and discusses a practical application example.

II. The classical Kalman filter

As already stated in [27], the Kalman filter is a widely known estimation algorithm, used to estimate the system state of a dynamical system [1], [28].

In this paper, a dynamical system is represented in the discrete-time form, since it is the most useful representation when dealing with digital signal processing and control:

$$\mathbf{x}_k = \mathbf{A}_{k-1}\mathbf{x}_{k-1} + \mathbf{B}_{k-1}\mathbf{u}_{k-1} \tag{1}$$

where $\mathbf{x}_k$ is the system state vector, containing the terms of interest of the system at the discrete time k; $\mathbf{u}_k$ is the vector containing any control input; $\mathbf{A}$ is the *state-transition* matrix, which applies the effect of each system state parameter at time $k-1$ on the system state at time k; and $\mathbf{B}$ is the *control-input* matrix, which applies the effect of each control input parameter in the vector $\mathbf{u}_k$ on the state vector [1], [28].

In many applications, the system state $\mathbf{x}_k$ is not directly accessible, but an output quantity $\mathbf{y}_k$ related to $\mathbf{x}_k$ is measurable. Let us suppose the following relationship between $\mathbf{x}_k$ and $\mathbf{y}_k$:

$$\mathbf{y}_k = \mathbf{H}_k\mathbf{x}_k \tag{2}$$

where $\mathbf{H}_k$ is the *transformation* matrix, that maps the state vector parameters into the measurement domain [1], [28].

It can be readily checked that, if the model were perfectly defined and the input and the initial conditions were known without uncertainty, the state evolution could be exactly determined. However, in the real world, both measurements and models are affected by uncertainty, and the estimation algorithm is therefore required to deal with uncertainties. The Kalman filter is the best-known algorithm that can be applied, under the assumption that both measurements and models are affected by random uncertainties that, if not correlated, may not have a Gaussian distribution as required by the original formulation of the Kalman filter. Thus, (1) and (2) can be rewritten as:

$$\mathbf{x}_k = \mathbf{A}_{k-1}\mathbf{x}_{k-1} + \mathbf{B}_{k-1}\mathbf{u}_{k-1} + \mathbf{w}_{k-1} \tag{3}$$

$$\mathbf{y}_k = \mathbf{H}_k\mathbf{x}_k + \mathbf{v}_k \tag{4}$$

where $\mathbf{w}_k$ is the vector containing the process noise terms for each parameter in the state vector. The process noise is assumed to be drawn from a zero mean Gaussian probability distribution (PDF) with covariance matrix $\mathbf{Q}_k$ [1], [28]. $\mathbf{v}_k$ is the vector containing the measurement noise terms for each observation in the measurement vector. Similarly to the process noise, the measurement noise is assumed to be zero mean Gaussian white noise with covariance matrix $\mathbf{R}_k$ [1], [28].

As recalled in [27], the aim of the Kalman filter is to estimate, at each time instant k, the state vector $\mathbf{x}_k$, from the observed measured vector $\mathbf{y}_k$, with the constraint that the state evolution must obey the dynamical system represented by (3) and (4).

The estimation process is composed by two steps, as summarized in Fig. 1: a prediction step, in which the *a priori* estimate of $\mathbf{x}_k$ is calculated starting from the previously-calculated estimate of $\mathbf{x}_{k-1}$, and an assimilation (or correction) step, in which the *a priori* estimate is combined with the observation of the output $\mathbf{y}_k$ in order to obtain the *a posteriori* best estimate. The filter is recursive and the two steps alternate.

In Fig. 1, the superscript f refers to the forecasts, that is, to the a priori estimates, while the superscript a refers to the a posteriori estimates. Further details about the theory of the Kalman filters can be found in the literature, for instance in [1], [29]. Let us only consider here the role played by the matrix gain $\mathbf{K}_k$, which depends on the covariance matrices $\mathbf{Q}_k$ and $\mathbf{R}_k$, that is, on the uncertainties associated to model and measurements.

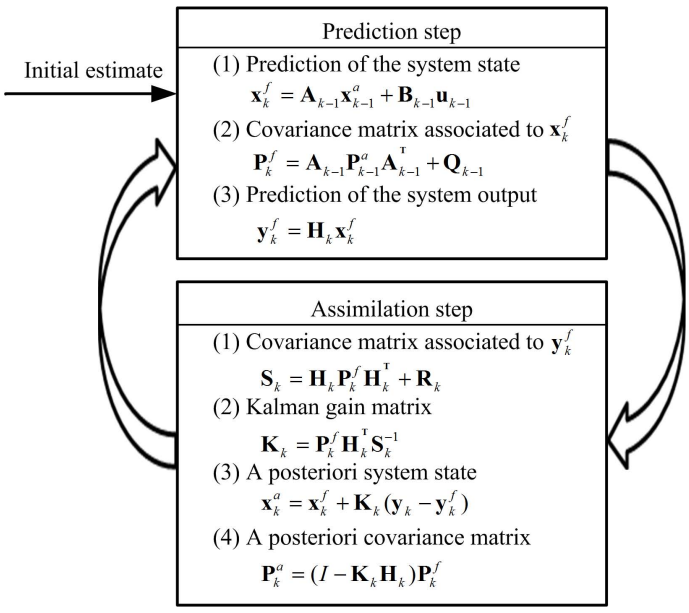

Fig. 1. Steps of the classical Kalman filter.

$\mathbf{K}_k$ represents the weight given to the correction of the *a priori* estimate because of the disagreement between the predicted and the actual outputs. Therefore, the values taken by the gain matrix depend on the reliability of the measurement result compared to that of the *a priori* estimate. If the measurement uncertainty (represented by matrix $\mathbf{R}_k$) is very high, $\mathbf{K}_k$ is very low. This reflects the fact that the measurement can't be trusted and, therefore, the a posteriori estimate will be very similar to the a priori estimate. On the contrary, if the measurement uncertainty is very low (i. e. $\mathbf{R}_k$ tends to zero), $\mathbf{K}_k$ becomes almost equal to $\mathbf{H}_k^{-1}$ and the a posteriori states will be very similar to the measurements.

It is therefore evident that an imprecise evaluation of the uncertainty of either the measurement result or the model, due to assumptions that do not represent the measurement uncertainty correctly, can lead to an incorrect assimilation step. This is the reason why, in the Author's opinion, the assumption of Gaussian white random noise might become too restrictive in most measurement applications and should be relaxed. The next section presents a possible way to extend the Kalman filter to the more general case where the noise contributions are not the only or the most relevant random contributions to uncertainty, not all random contributions can be correctly represented by normal probability distributions, and also non-random contributions to uncertainty, as the systematic ones, are present.

It is worth mentioning also the extended Kalman filter (EKF), which considers a non-linear relationship among the state variables and the measurements [30]. This paper considers the classical Kalman filter for the sake of simplicity, since the same approach as the one proposed here can be applied to the EKF.

III. The Kalman filter in the possibility domain

Before reformulating the classical Kalman filter into the possibility domain in terms of RFVs, it is necessary to briefly recall some definitions. The readers are addressed to the referenced documents for all mathematical proofs and details.

A. Possibility distributions and Random-Fuzzy variables

It has been shown [16]–[18] that a measurement result, together with the uncertainty contributions due to both random and non-random effects, including the systematic ones, affecting the measurement process, can be effectively represented by a Random-Fuzzy variable (RFV).

An RFV is composed by two different possibility distributions (PDs) (as shown in the lower plot of Fig. 2), where a PD is a convex function $r_X(x)$, such that $r : X \rightarrow [0, 1]$ and $sup_{x \in X} r_X(x) = 1$ [12].

The "internal PD" r^{int} (blue line, also shown in the upper plot of Fig. 2), represents the effects, on the measurement result, of the non-random contributions to uncertainty, while the "external PD" r^{ext} (pink line, lower plot) represents the effects, on the measurement result, of all uncertainty contributions.

The external PD is obtained by combining r^{int} with a "random PD" r^{ran} (central plot), which represents the effects of the random contributions to uncertainty only. This combination is mathematically obtained according to:

$$r_X^{\text{ext}}(x) = \sup_{x'} \; T_{min} \left[r_X^{\text{ran}}(x - x' + x^*), r_X^{\text{int}}(x') \right] \quad (5)$$

where x^* is the mode of r_X^{ran} and T_{min} is a fuzzy operator, called *min* t-norm and defined as $T_{min}[a, b] = \min(a, b)$ [31].

T_{min} belongs to the class of t-norms defined in the literature, that is, fuzzy operators obeying to specific mathematical rules [18], that can be used to combine PDs [32], [33]. Other t-norms that are useful for the combination of RFVs are the Frank and Dombi t-norm.

Hence, all uncertainty contributions, random and non-random, are represented together in a unique RFV, and their single effects are also represented, thus allowing to process the different contributions in a different way [11], [32], [34], according to their nature and the way they combine in the measurement procedure.

An RFV is built according to the available metrological information about the measured quantity X [11], [22], [34], [35]. r_X^{int} is generally obtained directly from the available information [34]; r_X^{ran} is generally obtained through a probability-possibility transformation [35], [36], according to the fact that the available information about random contributions is generally represented by a PDF. Finally, starting from r_X^{int} and r_X^{ran}, the "external PD" r^{ext} is obtained according to (5), as shown in [37].

When the combination of two RFVs, according to a relationship f, i. e. $C = f(C_1, C_2)$, is required, the following procedure is applied [11], [32]–[34], [37]:

- the joint random PD r_{C_1,C_2}^{ran} associated to the random PDs of C_1 and C_2, is evaluated by applying a Frank or a Dombi t-norm [38], [39];
- the joint internal PD r_{C_1,C_2}^{int}, associated to the internal PDs of C_1 and C_2, is evaluated by applying the t-norm that better represents the way the two contributions combine [38]. In particular, it has been proved that, when two contributions combine in a random way, the most suitable t-norm is a t-norm from the Frank [11] or Dombi families [38]; on the other hand, when two contributions combine in a non-random way, the most suitable t-norm is the $\min$ t-norm [11];
- the joint external PD r_{C_1,C_2}^{ext} is then obtained (starting from r_{C_1,C_2}^{int} and r_{C_1,C_2}^{ran}) by extending (5) to the joint PDs [37];
- the Zadeh extension principle (ZEP) is applied twice: to r_{C_1,C_2}^{int} and r_{C_1,C_2}^{ext}, thus obtaining the internal and external PDs respectively, associated to RFV $C = f(C_1, C_2)$.

As preliminary shown in [27], the described procedure can be simplified, thus reducing the computational burden, when function f is linear, for instance when two RFVs are added. Under this assumption, it is not necessary to build the joint external PD r_{C_1,C_2}^{ext} and the ZEP can be applied directly to r_{C_1,C_2}^{int} and r_{C_1,C_2}^{ran}, thus obtaining respectively the internal and random PDs associated to C. Then, the direct application of (5) allows one to evaluate the external PD and thus obtain the final RFV C.

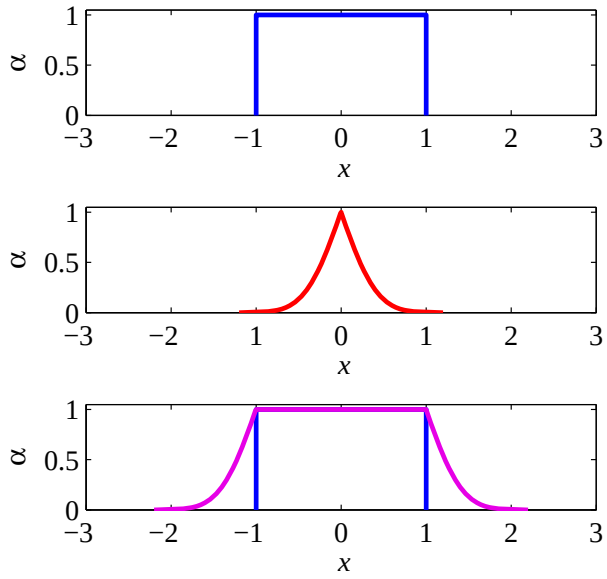

Fig. 2. Internal PD r_X^{int} (upper plot), random PD r_X^{ran} (central plot), final RFV (lower plot).

A PD can be also defined in terms of its α-cuts $X_\alpha = \{x \in X | r_X(x) \geq \alpha\}$. By definition, the α-cuts of a PD are closed intervals $X_\alpha = [x_1^\alpha, x_2^\alpha]$. When an RFV is considered, the α-cuts are confidence intervals of type 2 [18]. It can be proved that the α-cuts generalize the probabilistic concept of confidence interval [16], [18] and that the level of confidence associated to the α-cut at level α is $\gamma = 1 - \alpha$. Therefore, the support of an RFV (α-cut at $\alpha = 0$) represents the confidence interval at confidence level 1.

B. Variance and covariance of possibility distributions

In order to apply the above concepts to the Kalman filter theory described in Sec. II, it is necessary to define the mean value, the variance and covariance of a fuzzy variable. Definitions of crisp possibilistic mean value, crisp possibilistic variance and crisp possibilistic covariance of continuous PDs which are consistent with the ZEP can be found in [40].

Let us consider a fuzzy variable X, with associated possibility distribution $r_X(x)$, and let us denote its generic α-cut $X_\alpha = [x_1^\alpha, x_2^\alpha]$. Then, the crisp possibilistic mean value and variance of X are defined, respectively, as [40]:

$$M(X) = \int_0^1 \alpha \left(x_1^\alpha + x_2^\alpha\right) d\alpha \tag{6}$$

$$Var(X) = \frac{1}{2} \cdot \int_0^1 \alpha \left(x_2^\alpha - x_1^\alpha\right)^2 d\alpha \tag{7}$$

It is interesting to note that the crisp possibilistic mean value and variance of a linear combination of fuzzy numbers can be computed in a similar way as in the probability theory. In fact, if X and Y are two fuzzy numbers and a and b are two real numbers:

$$M(aX + bY) = a \cdot M(X) + b \cdot M(Y)$$

$$Var(aX+bY) = a^2 \cdot Var(X) + b^2 \cdot Var(Y) + 2 \cdot |ab| \, Cov(X, Y)$$

where $Cov(X, Y)$ is the crisp possibilistic covariance between X and Y and is defined as [40]:

$$Cov(X, Y) = \frac{1}{2} \cdot \int_0^1 \alpha \left(x_2^\alpha - x_1^\alpha\right) \left(y_2^\alpha - y_1^\alpha\right) d\alpha \tag{8}$$

The above equations are valid for continuous PDs. From the practical point of view, however, discrete PDs are employed, that is PDs defined on a finite number of α-cuts. Therefore, (6)-(8) have to be modified, according to the considered discretization. If N equally-spaced α levels are considered, (6)-(8) can be evaluated as:

$$M(X) = \frac{1}{N} \sum_{i=1}^{N} \alpha_i \left(x_1^{\alpha_i} + x_2^{\alpha_i}\right) \tag{9}$$

$$Var(X) = \frac{1}{2 \cdot N} \cdot \sum_{i=1}^{N} \alpha_i \left(x_2^{\alpha_i} - x_1^{\alpha_i}\right)^2 \tag{10}$$

$$Cov(X, Y) = \frac{1}{2 \cdot N} \cdot \sum_{i=1}^{N} \alpha_i \left(x_2^{\alpha_i} - x_1^{\alpha_i}\right) \left(y_2^{\alpha_i} - y_1^{\alpha_i}\right) \tag{11}$$

where $\alpha_i = \frac{1}{N-1} \cdot (i - 1)$. In the example shown in next Section IV, $N = 101$ is considered.

C. Kalman filter with RFVs

The definitions of RFVs given in Sec. III-A and the definitions of possibilistic variance and possibilistic covariance of PDs given in Sec. III-B allow us to extend, in a very straightforward way, the classical theory of Kalman filters in a possibilistic framework [27]. This allows us to apply the Kalman filter also when the possibilistic framework is used for expressing measurement uncertainty in a GUM-compliant way.

Since this means that the state variables, the input and the measured quantities are expressed by RFVs, without any restriction on their shape, we also have the advantage that no assumptions are needed on the distribution of the random contributions to uncertainty, and both systematic and random contributions to uncertainty can be considered.

Let us consider again Fig. 1, which shows the recursive prediction and assimilation steps of the classical, probabilistic Kalman filter. In the prediction step, the *a priori* state is evaluated according to the system model, starting from the previous *a posteriori* state; while the *a priori* output is obtained from the *a priori* state, according to the transformation matrix $\mathbf{H}_k$. In the assimilation step, the *a posteriori* state is evaluated according to the *a priori* state, the *a priori* output and the actual measured value of the output. In these equations, we refer to crisp values. Their associated uncertainty, which depends on the model and measurement uncertainties (represented respectively by the covariance matices $\mathbf{Q}_k$ and $\mathbf{R}_k$), are evaluated separately (see the equations in Fig. 1).

When the possibility domain is considered, there is no need to consider different variables and equations to represent and propagate a variable and its uncertainty since RFVs consider all uncertainty contributions and t-norms consider the combination of RFVs. This means that different kinds of

uncertainty contributions, with whichever distribution, can be considered and propagated [18].

Thanks to the use of RFVs, model uncertainty can be included directly in the prediction of the system state. In fact, it is possible to suppose that the state-transition matrix (matrix $\mathbf{A}_k$) is not simply a matrix of crisp values, but a matrix of RFVs which also include model uncertainty on the evaluation of the state-transition matrix. Let us call this matrix $\mathbf{A*}_k$. Similarly, it is possible to suppose that the control-input matrix (matrix $\mathbf{B}_k$) is not simply a matrix of crisp values, but a matrix of RFVs which also include model uncertainty on the evaluation of the control-input matrix. Let us call this matrix $\mathbf{B*}_k$.

Under this assumption, the prediction of the system state can be written, in the possibility domain, as:

$$\mathbf{X}_k^f = \mathbf{A*}_{k-1}\mathbf{X}_{k-1}^a + \mathbf{B*}_{k-1}\mathbf{U}_{k-1} \tag{12}$$

where the vector of the control input can be a vector of crisp values ($\mathbf{u}_k$) or a vector of RFVs ($\mathbf{U}_k$) if uncertainty contributions are also associated to the control inputs. In (12), symbol $\mathbf{U}_k$ is used, to consider the more general case.

According to (12), by applying the mathematics of RFVs [18], because of the presence of RFVs in $\mathbf{A*}_k$ and $\mathbf{B*}_k$, $\mathbf{X}_k^f$ is surely a vector of RFVs, associated to the *a priori* system state. This means that RFVs in vector $\mathbf{X}_k^f$ are already affected by the model uncertainty. So, (12) includes both steps (1) and (2) in the prediction step of Fig. 1.

Since $\mathbf{X}_k^f$ is a vector of RFVs, the a priori output vector $\mathbf{Y}_k^f$ is a vector of RFVs as well:

$$\mathbf{Y}_k^f = \mathbf{H}_k\mathbf{X}_k^f \tag{13}$$

where $\mathbf{H}_k$ is the same transformation matrix defined in (2). Again, (13) includes both phase (3) of the prediction step and phase (1) of the assimilation step in Fig. 1.

Measurement uncertainty is also considered directly on the output measured values $\mathbf{y}_k$, so that a vector of RFVs $\mathbf{Y}_k$ is obtained. This allows us to evaluate the *a posteriori* system state according to:

$$\mathbf{X}_k^a = \mathbf{X}_k^f + \mathbf{K}_k^{POS}\left(\mathbf{Y}_k - \mathbf{Y}_k^f\right) \tag{14}$$

where $\mathbf{K}_k^{POS}$ is again a gain matrix, with the same meaning as the one given in Sec. II, but evaluated in a different way, according to the possibilistic definitions of variance and covariance given in Sec. III-B. Let us call $\mathbf{K}_k^{POS}$ the *possibilistic gain matrix*.

In order to define $\mathbf{K}_k^{POS}$, let us first of all consider again the definition of the gain matrix in the probability domain:

$$\mathbf{K}_k = \mathbf{P}_k^f\mathbf{H}_k^T\left(\mathbf{H}_k\mathbf{P}_k^f\mathbf{H}_k^T + \mathbf{R}_k\right)^{-1} \tag{15}$$

where

$$\mathbf{P}_k^f = \mathbf{A}_{k-1}\mathbf{P}_{k-1}^a\mathbf{A}_{k-1}^T + \mathbf{Q}_{k-1} \tag{16}$$

is the covariance matrix associated to $\mathbf{X}_k^f$. Hence, in the probability domain, $\mathbf{K}_k$ is built considering the model (matrices $\mathbf{A}_k$ and $\mathbf{H}_k$) and the noise (matrices $\mathbf{Q}_k$ and $\mathbf{R}_k$) and requires, at each step k, the evaluation of (16).

On the other hand, in the possibility domain, it is possible to evaluate the covariance matrix associated to $\mathbf{X}_k^f$, by simply applying the definition of variance and covariance given in Sec. III-B.

Not to confuse the meaning of the symbols, let us denote this matrix with a different symbol than $\mathbf{P}_k^f$; let us name it: $\mathbf{C}_{\mathbf{X}_k^f}$. If $\mathbf{X}_k^f$ is a vector of dimension n

$$\mathbf{X}_k^f = \left[X_1^f, X_2^f, ..., X_n^f\right],$$

then it is:

$$\mathbf{C}_{\mathbf{X}_k^f} = \begin{bmatrix} Var(X_1^f) & Cov(X_1^f, X_2^f) & ... & Cov(X_1^f, X_n^f) \\ Cov(X_2^f, X_1^f) & Var(X_2^f) & ... & Cov(X_1^f, X_n^f) \\ ... & ... & ... & ... \\ Cov(X_n^f, X_1^f) & Cov(X_n^f, X_2^f) & ... & Var(X_n^f) \end{bmatrix} \tag{17}$$

where subscript k has been omitted for the sake of simplicity.

It is worth noting that $\mathbf{C}_{\mathbf{X}_k^f}$ is again a matrix of crisp values, but obtained in a different way than $\mathbf{P}_k^f$.

Similarly, it is possible to evaluate the covariance matrix associated to $\mathbf{Y}_k$. Let us denote this matrix $\mathbf{C}_{\mathbf{Y}_k}$. Hence, the possibilistic gain matrix can be evaluated as:

$$\mathbf{K}_k^{POS} = \mathbf{C}_{\mathbf{X}_k^f}\mathbf{H}_k^T\left(\mathbf{H}_k\mathbf{C}_{\mathbf{X}_k^f}\mathbf{H}_k^T + \mathbf{C}_{\mathbf{Y}_k}\right)^{-1} \tag{18}$$

A further short discussion is necessary about $\mathbf{K}_k^{POS}$. In fact, as recalled in Sec. III-A, RFVs are defined by three different PDs: the internal, the random and the external one. It follows that the definition of variance and covariance can be applied to all these PDs, thus leading to different values and, hence, to different possible values for $\mathbf{K}_k^{POS}$. In particular, when Eqs. (10) and (11) are applied to the internal PDs of the *a priori* RFVs, a value $\mathbf{K}_k^{\text{int}}$ is obtained. Similarly, when the random PDs are considered, a value $\mathbf{K}_k^{\text{ran}}$ is obtained, and when the external PDs are considered, a value $\mathbf{K}_k^{\text{ext}}$ is obtained. Since these values are generally different and may provide different results for $\mathbf{X}_k^a$, the correct selection of the value to be used in (14) is a critical step. This can be done by recalling the role of the gain matrix, as discussed in Sec. II. According to that discussion, it is reasonable to consider, for the evaluation of the possibilistic gain matrix, the overall uncertainty, which is taken into account by the external PDs of the RFVs. Therefore, $\mathbf{K}_k^{POS} = \mathbf{K}_k^{\text{ext}}$ is considered in (14).

IV. An application example

A. The experimental set-up

To give an experimental validation to the proposed possibilistic Kalman filter, the dynamical model already employed in [41] is considered: a rotating DC, shunt connected motor, of which we want to estimate the angular position ϑ. The angular position is also the output of the system, which, of course, depends on the motor speed. An encoder (Wachendorff WDG 58B) is mechanically coupled to the motor shaft, and provides 4096 PPR, that is, 4096 pulses for every revolution of the motor shaft. The motor and the experimental setup already employed in [41] are shown, respectively, in Figs. 3 and 4. According to the measurements and the discussion in [41], a

Fig. 3. The employed motor

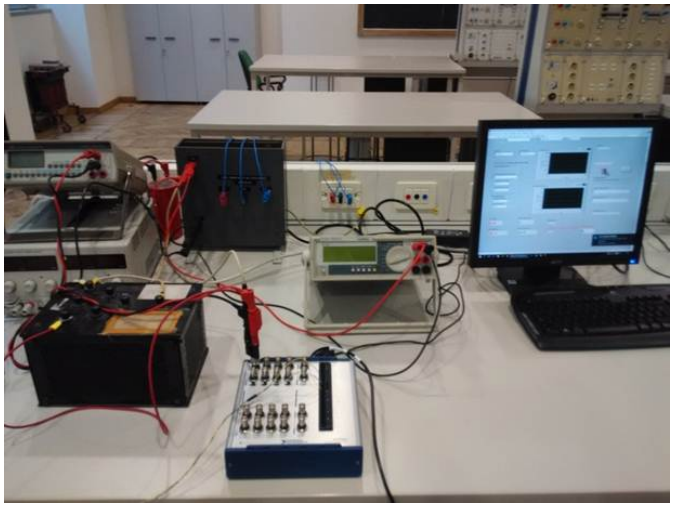

Fig. 4. The experimental setup

linear relationship has been found between the applied voltage and the rotation speed :

$$\omega = c_1 \cdot v + c_2 \tag{19}$$

In the considered example, a constant voltage is applied to the motor. Therefore, at steady state, the motor rotation speed ω is constant.

Eq. (19) allows us to write the following motor model:

$$\Delta\vartheta = \omega \cdot \Delta t = (c_1 \cdot v + c_2) \cdot \Delta t \tag{20}$$

where $\Delta\vartheta$ is the variation of the angular position in the time period Δt.

B. Estimation of the uncertainty contributions

Different experiments have been considered and two groups of data have been acquired.

1) Coefficients uncertainty estimation: In the first experiment, different voltage values have been applied to the motor and, for each of these values, both the voltage and the corresponding rotation speed have been acquired with an ADC board (NI-USB-6356). This first group of data has allowed us to obtain coefficients c_1 and c_2 in Eq. (19) for the considered motor, as detailed in [41]. Furthermore, the evaluation of the uncertainties associated to c_1 and c_2, according to the experimental data, has also allowed us to built RFVs C_1 and C_2 associated to these coefficients [41], as shown in Fig. 5.

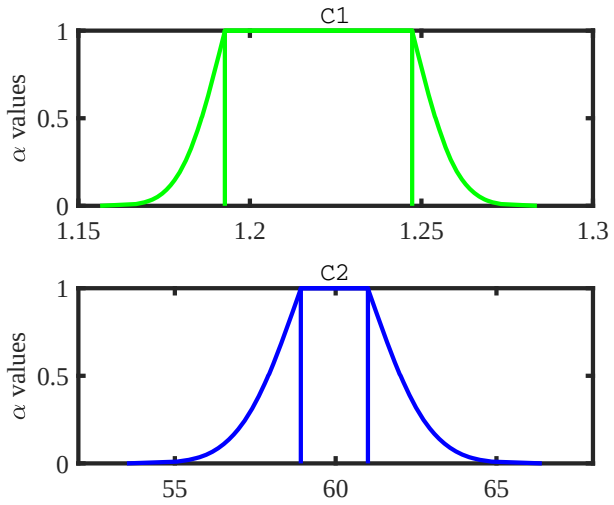

Fig. 5. RFVs C_1 and C_2.

Therefore, Eqs. (19) and (20) can be rewritten in terms of RFVs, as:

$$\Omega = C_1 \cdot V + C_2 \tag{21}$$

$$\Delta\Theta = \Omega \cdot \Delta t = (C_1 \cdot V + C_2) \cdot \Delta t \tag{22}$$

2) Voltage and angular position uncertainty estimation: In the second experiment, a constant voltage value has been applied to the motor and the ADC board is used to acquire both the supply voltage and the pulses of the encoder. In particular, 8192 encoder pulses have been acquired by the digital channel of the ADC board and the pulse periods T_{pp}, that is the time interval between one pulse of the encoder and the successive one, has been evaluated by a dedicated VI. This number (8192) has been chosen because it corresponds exactly to two motor revolutions, since, as already stated, the encoder provides 4096 pulses per revolution. On the other side, from the analog channel of the ADC board, 100000 voltage samples have been acquired at a sampling frequency $f_s = 1$ MHz.

Fig. 6 shows a screen-shot of the dedicated VI, when the applied voltage is 150 V. The graph of the acquired voltage is displayed, together with its mean value and standard deviation, and the graph of 256 measured values T_{pp_i} of the pulse period is also displayed. The figure shows how the vibration of the encoder, caused by the intrinsic vibrations of the motor and the possible residual inaccuracy in the link alignment, leads to a variability of the measured pulse period T_{pp}, which hence is not constant.

2a) Voltage uncertainty estimation: The voltage samples allow us to determine the voltage applied to the motor. In particular, because of the inertia of the motor, the motor rotates according to the mean value of the applied voltage and is not

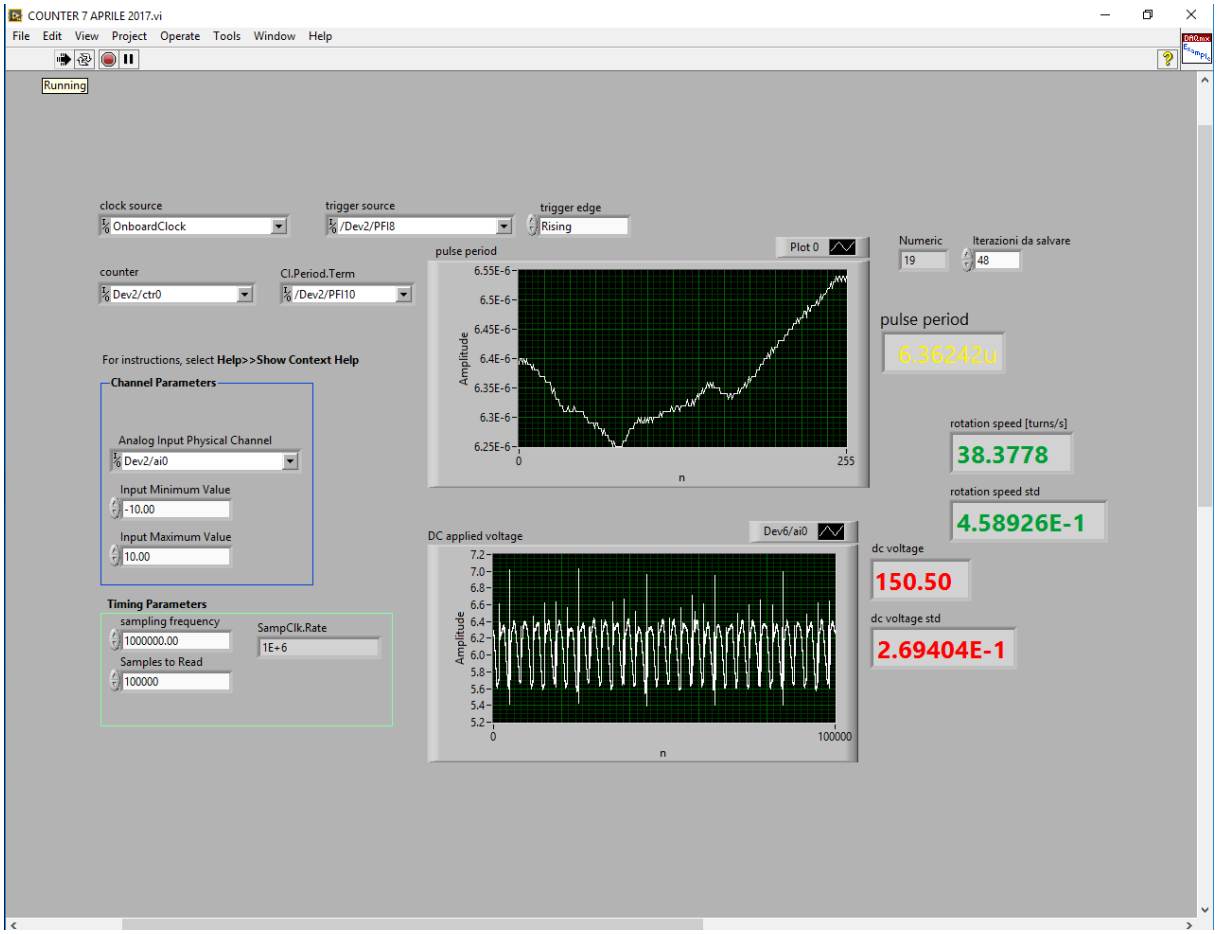

Fig. 6. Dedicated VI. The upper graph shows the measured pulse period over 256 pulses, which correspond to $\frac{1}{16}$ of turn. The lower graph shows the acquired voltage.

influenced by the voltage ripple. Therefore, the voltage mean value over two revolutions of the motor is considered.

The time period for two revolutions of the motor is given by:

$$\Delta t_{TOT} = \sum_{i=1}^{8192} T_{pp_i} = 52.27 \text{ ms}$$

and, since the sampling frequency is $1MHz$, 52270 voltage samples are acquired over period Δt_{TOT}. According to the acquired voltage samples, the mean value of the first 52270 samples provides a voltage mean value $V_m = 150.39$ V.

Furthermore, two different assumptions are considered.

- According to the acquired samples, the measurement uncertainty associated to the mean value is negligible with respect to the uncertainty contributions associated to c_1 and c_2. Therefore, the considered supply voltage V_m is supposed to be a crisp value, without uncertainty.
- In order to study how the uncertainty contributions on the supply voltage may influence the estimation of the system state, both random and systematic contributions are assumed, so that the supply voltage is no more expressed by a crisp value without uncertainty, as in the previous case, but by an RFV centered on V_m.
  Different values of the uncertainty contributions have been considered, in order to see their impact on the final results. In particular, the internal PD of the voltage has been considered rectangular, with a width ranging from $\pm 1\%$ to $\pm 10\%$ of V_m; while the random PD has been considered the PD obtained from a normal PDF, having a standard deviation ranging from 1 V to 10 V.

2b) Angular position uncertainty estimation: The measured pulse periods are used to build the RFVs associated to the measured angular position. First of all, the 8192 measured values T_{pp_i} are divided into 32 groups of 256 measurements each. This assumption allows us to obtain 32 possible steps for the Kalman filter, at well-separated expected angular positions. Let us then consider, for every time instant t_k, the relationship between the measured pulse period T_{pp} and the measured angular position ϑ_k in radians:

$$\vartheta_k = \frac{2\pi}{4096 \cdot T_{pp}} \cdot t_k \tag{23}$$

From this equation, it is possible to obtain the expected, theoretical values of the angular position by considering that, due to the inertia of the motor, when the supply voltage shows a constant mean value, the motor rotation speed is constant (at steady state), the pulse period $T_{pp}^{expected}$ is constant and the angular position uniformly increases as the time increases. Under this assumption, it is possible to consider, in (23), $T_{pp} =$

$T_{pp}^{expected}$ and $t_k = 256 \cdot k \cdot T_{pp}^{expected}$; thus leading to:

$$\vartheta_k^{expected} = \frac{2\pi \cdot 256 \cdot k \cdot T_{pp}^{expected}}{4096 \cdot T_{pp}^{expected}} = \frac{\pi}{8} \cdot k \qquad (24)$$

as reported in the second column of Table I.

The increment of the angular position in two successive steps is constant and is given by: $\Delta\vartheta^{expected} = \frac{\pi}{8} = 0.3927$.

On the other hand, because of the different measured values T_{pp_i}, the measured angular positions differ from the expected ones: $\vartheta_k \neq \vartheta_k^{expected}$. In order to evaluate the measured ϑ_k (as reported in the third column of Table I), (23) is applied under the following assumptions:

- since 8192 measured values of the pulse period are taken:

$$T_{pp} = \bar{T}_{pp} = \frac{1}{8192} \sum_{i=1}^{8192} T_{pp_i} = 6.38\mu\text{s}$$

- since the 8192 measured values are divided into 32 groups of 256 measurements each:

$$t_k = \sum_{i=1}^{256 \cdot k} T_{pp_i}$$

Furthermore, the variability of the 8192 measured values T_{pp_i} allows us also to associate a measurement uncertainty to the measured angular positions ϑ_k, thus obtaining the corresponding RFVs Θ_k. First of all, the statistical analysis of the measured T_{pp_i} values has confirmed that they are not affected by any bias but only by random contributions. Therefore, RFVs Θ_k obtained by the experimental measurements have nil internal PDs and only show random PDs. Moreover, their variability over the 8192 values does not differ from their variability over the considered 32 steps. Therefore, it is reasonable to assume that the uncertainty associated to each measured value remains constant.

In particular, the distribution of the measured values is approximately normal, with standard deviation $\sigma_{T_{pp}} = 0.12\mu$s, hence, from Eq. (23):

$$\sigma_{\theta_k} = \sigma_\theta = \frac{2\pi}{4096 \cdot \bar{T}_{pp}} \cdot 256 \cdot \sigma_{T_{pp}} = 0.0072 \qquad (25)$$

From this value, and applying the probability-possibility transformation [18], RFVs Θ_k can be built. Since σ_θ is independent from k, it follows that all RFVs have the same shape and width, and only their mean values change, according to the measured values reported in the third column of Table I.

However, in order to study the effect on the estimation of some systematic contributions to uncertainty on the measured values, a further case study is also considered, by assuming that the measured values are also affected by systematic contributions to uncertainty. In particular, an internal, rectangular PD of width $\pm 0.1\%$ of the measured value is added to RFVs Θ_k. This will be shown in Sec. IV-D.

C. Application of the possibilistic Kalman filter

According to the theoretical considerations in Sec. III-C, the equations can be simplified for a time-invariant system, with only one state variable, one input variable and one output variable, as:

$$X_k^f = A^* \, X_{k-1}^a + B^* \, U_{k-1} \qquad (26)$$

$$Y_k^f = h X_k^f \qquad (27)$$

$$X_k^a = X_k^f + k_k^{POS} \left(Y_k - Y_k^f \right) \qquad (28)$$

$$k_k^{POS} = \frac{c_{X_k^f} \cdot h}{h^2 \cdot c_{X_k^f} + c_{Y_k}} \qquad (29)$$

If we now consider that the system state is the angular position, the input of the system is the voltage supply and the output of the system is again the angular position, we get the following equations:

$$\Theta_k^f = \Theta_{k-1}^a + (C_1 \cdot V_k + C_2) \, \Delta t_k \qquad (30)$$

$$Y_k^f = \Theta_k^f \qquad (31)$$

$$\Theta_k^a = \Theta_k^f + k_k^{POS} \left(\Theta_k - \Theta_k^f \right) = \Theta_k^f \left(1 - k_k^{POS} \right) + k_k^{POS} \Theta_k \qquad (32)$$

$$k_k^{POS} = \frac{c_{\Theta_k^f}}{c_{\Theta_k^f} + c_{\Theta_k}} \qquad (33)$$

where Θ_k^f and Θ_k^a are the *a priori* and *a posteriori* estimated RFVs associated to the angular position; Θ_k is the measured value; V_k is the RFV associated to the voltage supply, C_1 and C_2 are the RFVs associated to the motor model; Δt_k is the time interval between two consecutive steps; and k_k^{POS} is the possibilistic gain, where, according to (17), $c_{\Theta_k^f}$ is

TABLE I
ANGULAR POSITIONS AT THE FIRST THIRTY-TWO ITERATIONS [rad].

time step	Expected θ	Measured θ
1	0.3927	0.392
2	0.7854	0.778
3	1.1781	1.174
4	1.5708	1.575
5	1.9635	1.958
6	2.3562	2.355
7	2.7489	2.746
8	3.1416	3.134
9	3.5343	3.526
10	3.9270	3.925
11	4.3197	4.315
12	4.7124	4.707
13	5.1051	5.099
14	5.4978	5.491
15	5.8905	5.896
16	6.2832	6.289
17	6.6759	6.681
18	7.0686	7.069
19	7.4613	7.461
20	7.8540	7.852
21	8.2467	8.247
22	8.6394	8.633
23	9.0321	9.024
24	9.4248	9.414
25	9.8175	9.806
26	10.2102	10.20
27	10.6029	10.60
28	10.9956	10.99
29	11.3883	11.38
30	11.7810	11.77
31	12.1737	12.17
32	12.5664	12.57

the possibilistic variance of Θ_k^f and c_{Θ_k} is the possibilistic variance of Θ_k.

By comparing (30)-(31) with (26)-(27), and according to the definition of t_k given in the previous section, it follows that:

- $A^* = 1$;
- $B^* = C_1 \cdot V_k + C_2$, where C_1 and C_2 are the RFVs shown in Fig. 5;
- $h = 1$;
- $U_{k-1} = \Delta t_k = t_k - t_{k-1} = \sum_{i=1+256\cdot(k-1)}^{256\cdot k} T_{pp_i}$

To start the possibilistic KF recursive procedure, it is therefore necessary to set the initial condition, that is to build RFV Θ_0^a, associated to the initial angular position, and to build RFVs V_k and Θ_k.

As for the initial angular position, it is convenient to assume that $\Theta_0^a = 0$, since the initial position of the motor can be considered as the zero position, with no uncertainty. This does not affect the general validity of the proposed method, since any other RFV could be assigned to the initial value.

On the other hand, as far as V_k and Θ_k are concerned, according to the considerations about the uncertainty contributions and the discussion reported in previous Sec. IV-B, three different case studies are considered.

1) **CASE A.** The voltage supply is a constant value, equal to V_m. The measured values of the angular positions are affected by only the random contributions, as obtained by the experimental measurements, as shown in previous Sec. IV-B. A normal PDF with standard deviation σ_ϑ, given by (25), has been considered. Therefore, in this case, RFV Θ_k is centered on the measured value θ_k (third column in Table I), has nil internal PD and a random PD obtained from the assumed normal PDF (by applying the probability possibility transformation [18], [36], [42]).
2) **CASE B.** The measured values of the angular positions are affected by only the random contributions, as obtained by the experimental measurements, as shown in previous Sec. IV-B. Therefore, RFV Θ_k is built according to the same considerations as for CASE A. On the other hand, uncertainty contributions are added to the voltage supply. In particular, both random and systematic contributions are assumed. A rectangular internal PD is considered, whose width is a percentage p of V_m; a from-gaussian random PD is considered, with standard deviation σ. Hence, in (30), V_k is an RFV, constant with k, centered on V_m. Different values of p and σ are considered, to verify how the different uncertainty contributions on the voltage supply influence the results of the Kalman filter. The results are shown in next Sec. IV-D.
3) **CASE C.** The voltage supply is an RFV, as explained in previous CASE B. On the other hand, systematic contributions are added to the angular positions measured values. Therefore, in this case, RFV Θ_k is a complete RFV, centered on the measured value θ_k, with internal rectangular PD with width $\pm 0.1\%$ of the measured value, and with a random PD obtained from the assumed normal PDF, as explained for CASE A.

D. Results and comparison

In this section, the results obtained in the three different case studies are shown and discussed.

In particular, Fig. 7 shows some of the steps of the Kalman filter estimation for CASE A. For each of the reported steps, the green lines represent the obtained *a priori* RFVs (Θ_k^f), the cyan lines represent the RFVs associated to the measurements (Θ_k) and the red lines represents the obtained *a posteriori* RFVs (Θ_k^a). Fig. 8 shows the width of the α-cut at level of confidence 0.95% of the a posteriori RFVs in all 32 steps, and the effects (on these RFVs) of the systematic and random contributions to uncertainty. In particular, for each step k, the difference between the obtained a posteriori RFV and the expected angular position (Θ_k^a - $\theta_k^{expected}$) is evaluated and then the α-cut at level of confidence 0.95% is reported. This difference has been evaluated because, otherwise, the uncertainties could not be appreciated in the graph. In this figure, for each step k, the whole interval (delimited by the external stars) is the whole α-cut, while the smaller interval, delimited by the two internal stars, shows the effect of the systematic contributions only.

In this CASE A, the only systematic contributions are the ones associated to coefficients C_1 and C_2, that is to model uncertainty. Therefore, it can be stated that these contributions do not affect too much the *a posteriori* RFVs Θ_k^a, while the random contributions, which are present both in the model and measurement uncertainty prevail.

It can be also noted that the implemented Kalman filter does efficiently improve the estimates. Indeed, the relative width, with respect to the mean value, of the α-cut at $\alpha = 0.05$ (which corresponds to a 95% level of confidence) of RFV θ^a reduces, from the initial value of 6.6% of step 1, to 0.4% of step 16 and 0.2% of step 32.

Fig. 9 shows some of the steps of the Kalman filter estimation for CASE B. In particular, to obtain this figure, $\sigma = 3\text{V}$ and $p = \pm 2\%$ of the voltage value have been considered. The meaning of the red-green-cyan lines is the same as in Fig. 7. Fig. 10 shows the width of the α-cut at level of confidence 0.95% of the a posteriori RFVs in all the 32 steps in the case of Fig. 9. As in Fig. 8, the difference Θ_k^a - $\theta_k^{expected}$ is reported, for the same reasons.

By comparing this figure with Fig. 8, it can be noted that the two figures show very similar results. This means that the uncertainty contributions that have been added on the voltage supply have little effect on the results. In order to study more in depth this phenomenon, further simulations have been performed, with different uncertainty values. In particular, Fig. 11 shows the results obtained with $\sigma = 10\text{V}$ and $p = \pm 10\%$ of the measured value.

It can be noted that Figs. 11 and 10 are very similar, thus confirming that the effect on the obtained results of the uncertainty values on the voltage supply are negligible with respect to the effect of the other uncertainty contributions.

This is also confirmed by the relative widths of the α-cuts at a 95% level of confidence, that decrease from 7.0% of step 1 to 0.4% of step 16 and 0.2% of step 32.

Fig. 12 shows some of the steps of the Kalman filter for CASE C. As far as the voltage supply is concerned, it is

again: $\sigma = 3\text{V}$ and $p = \pm 2\%$. As far as the measured angular position is concerned, a standard deviation σ_θ and a systematic contribution $\pm 0.1\%$ of the measured value have been considered. The meaning of the red-green-cyan lines is the same as in Fig. 7. Fig. 13 shows the width of the α-cut at level of confidence 0.95% of the a posteriori RFVs in all the 32 steps in the case of Fig. 12. As in Fig. 8, the difference $\Theta_k^a - \theta_k^{expected}$ is reported, for the same reasons.

It can be noted how a systematic contribution on the measured values Θ_m affects the obtained results. Even if a quite small value has been considered in this simulation ($\pm 0.1\%$), it causes the width of the obtained RFVs to increase as k increases.

As expected, the systematic effect becomes the dominant contribution to uncertainty after a few iterations of the filter, since a systematic deviation on the position propagates and amplifies in time.

This confirms the importance of considering all contributions to uncertainty, since this example proves that neglecting even a small systematic contribution may lead to a dramatic underestimation of uncertainty.

V. Conclusion

This paper has shown how the classical Kalman filter can be re-defined by modeling the uncertainty contributions in the possibility domain in a GUM-compliant way, in terms of RFVs.

The main advantage of the proposed re-definition in the possibility framework is that different contributions to uncertainty – random with different PDFs and systematic – can be considered, represented and combined in a suitable, GUM-compliant way when the Kalman filter is used in measurement applications.

The paper has derived, according to the available mathematics of the RFVs, the equations that implement the proposed Kalman filter in the possibility domain and has proposed and experimental validation with a simple, though significant application, proving that different contributions to measurement uncertainty can be effectively considered and processed. The obtained results prove that the proposed method does efficiently take into account measurement uncertainty within the framework considered by the standard reference documents in metrology. It can be then considered as a suitable alternative to other implementations of the Kalman filter, where, as in all metrological applications, the "best" approach can be defined only in terms of the relevant available information, as proved in [11].

As already stated, this approach has the merit of being compliant with the uncertainty concept considered by the GUM [4], although it evaluates uncertainty under a different mathematical framework [16], [18].

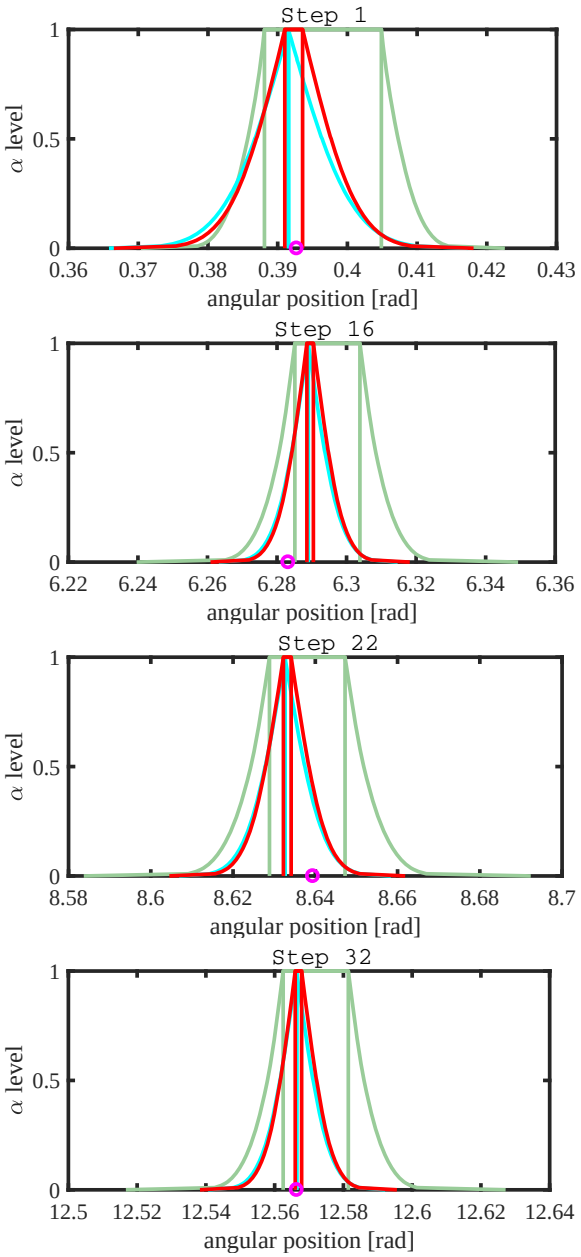

Fig. 7. Four step of the Kalman filters when the voltage supply is constant and the measured angular positions are affected by random uncertainty contributions only (CASE A). The green lines represent the obtained *a priori* RFVs (Θ_k^f), the cyan lines represent the RFVs associated to the measurements (Θ_k) and the red lines represents the obtained *a posteriori* RFVs (Θ_k^a). The pink circles represent the expected angular position.

References

[1] R. E. Kalman. A new approach to linear filtering and prediction problems. *J. Basic Eng.*, 82(1):35–45, 1960.

[2] E. A. Wan and R. Van Der Merwe. The unscented kalman filter for nonlinear estimation. In *Proceedings of the IEEE 2000 Adaptive Systems for Signal Processing, Communications, and Control Symposium (Cat. No.00EX373)*, pages 153–158, Oct 2000.

[3] L. Angrisani, A. Baccigalupi, and R. Schiano Lo Moriello. Ultrasonic time-of-flight estimation through unscented kalman filter. *IEEE Transactions on Instrumentation and Measurement*, 55(4):1077–1084, Aug 2006.

[4] JCGM 100:2008. *Evaluation of Measurement Data – Guide to the Expression of Uncertainty in Measurement, (GUM 1995 with minor corrections)*. Joint Committee for Guides in Metrology, 2008.

[5] W. Wei, S. Gao, Y. Zhong, C. Gu, and A. Subic. Random weighting estimation for systematic error of observation model in dynamic vehicle navigation. *International Journal of Control, Automation and Systems*, 14(2):514–523, April 2016.

[6] Y. Yang, N. Rees, and T. Chuter. Reduction of encoder measurement errors in ukirt telescope control system using a kalman filter. *IEEE Transactions on Control Systems Technology*, 10(1):149–157, Jan 2002.

[7] B. Noack, V. Klumpp, and U. D. Hanebeck. State estimation with

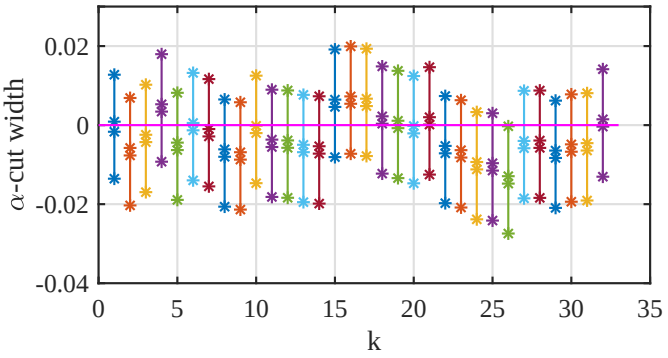

Fig. 8. Evolution of the α-cut widths at confidence level 0.95 for all 32 steps in the case shown in Fig. 7.

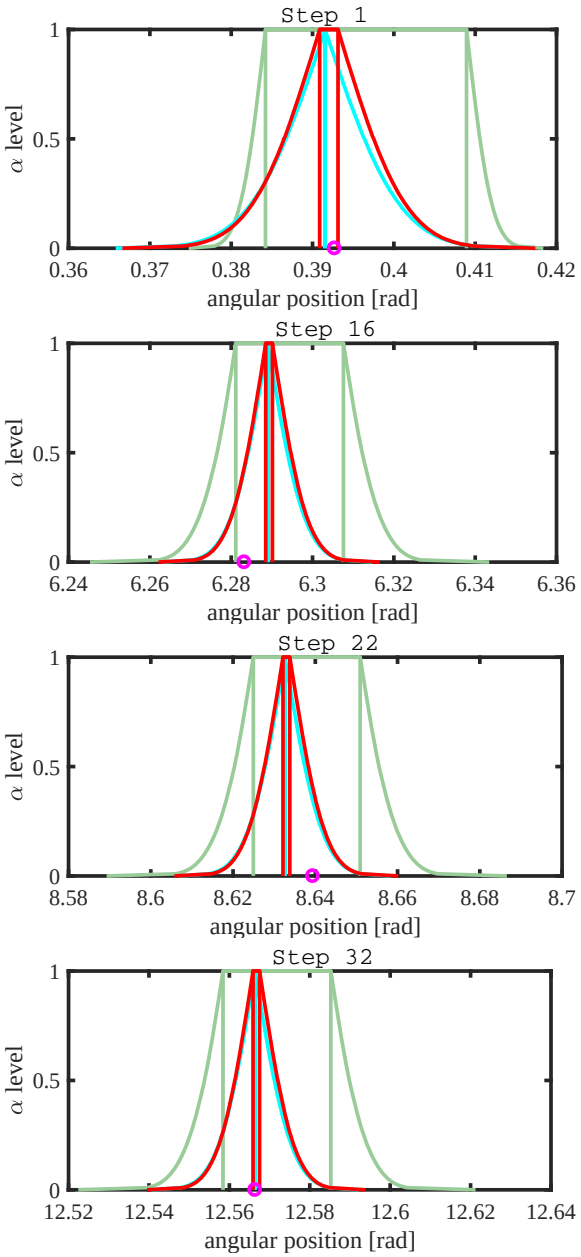

Fig. 9. Four step of the Kalman filters when random and systematic contributions are added to the voltage supply and the measured angular positions are affected by random uncertainty contributions only (CASE B). The green lines represent the obtained *a priori* RFVs (Θ_k^f), the cyan lines represent the RFVs associated to the measurements (Θ_k) and the red lines represents the obtained *a posteriori* RFVs (Θ_k^a). The pink circles represent the expected angular position.

sets of densities considering stochastic and systematic errors. In 12^{th} *International Conference on Information Fusion*, Seattle, WA, USA, July 6-9, 2009.

[8] I. Neumann and H. Kutterer. A kalman filter extension for the analysis of imprecise time series. In *EUSIPCO 2007*, Poznan, Poland, September 3-7, 2007.

[9] M. Urbanski and J. Wasowsky. Fuzzy approach to the theory of measurement inexactness. *Measurement, Elsevier Science*, 34:67–74, 2003.

[10] G. Mauris. Expression of measurement uncertainty in a very limited knowledge context: A possibility theory-based approach. *IEEE Trans. Instrum. Meas.*, 56(3):731–735, 2007.

[11] A. Ferrero and S. Salicone. A comparison between the probabilistic and possibilistic approaches: The importance of a correct metrological information. *IEEE Trans. Instrum. Meas.*, 67(3):607–620, March 2018.

[12] G. Shafer. *A Mathematical Theory of Evidence*. Princeton Univ. Press, Princeton, NJ, USA, 1976.

[13] L. A. Zadeh. Fuzzy sets as a basis for a theory of possibility. *Fuzzy Sets and Systems*, 1(1):3–28, 1978.

[14] G. Mauris, L. Berrah, L. Foulloy, and A. Haurat. Fuzzy handling of measurement errors in instrumentation. *IEEE Trans. Instrum. Meas.*, 49(1):89–93, 2000.

[15] G. Mauris, V. Lasserre, and L. Foulloy. A fuzzy approach for the expression of uncertainty in measurement. *Measurement*, 29:165–177, 2001.

[16] A. Ferrero and S. Salicone. Uncertainty: Only one mathematical approach to its evaluation and expression? *IEEE Trans. Instrum. Meas.*, 61(8):2167–2178, 2012.

[17] A. Ferrero and S. Salicone. The random-fuzzy variables: a new approach for the expression of uncertainty in measurement. *IEEE Trans. Instrum. Meas.*, 53(5):1370–1377, 2004.

[18] S. Salicone and M. Prioli. *Measurement Uncertainty within the Theory of Evidence*. Springer series in Measurement Science and Technology. Springer, New York, NY, USA, 2018.

[19] F. Matìa, A. Jiménez, B. M. Al-Hadithi, D. Rodrìguez-Losada, and R. Galán. The fuzzy kalman filter: State estimation using possibilistic techniques. *Fuzzy Sets and Systems*, 157(16):2145 – 2170, 2006.

[20] M. Oussalah and J. De Schutter. Possibilistic kalman filtering for radar 2d tracking. *Information Sciences*, 130(1):85 – 107, 2000.

[21] JCGM 200:2012. *International Vocabulary of Metrology – Basic and General Concepts and Associated Terms (VIM 2008 with minor corrections)*. Joint Committee for Guides in Metrology, 2012.

[22] A. Ferrero and S. Salicone. The construction of random-fuzzy variables from the available relevant metrological information. *IEEE Trans. Instrum. Meas.*, 58(2):1149–1157, 2009.

[23] Q. Zhu, Z. Jiang, Z. Zhao, and H. Wang. Uncertainty estimation in measurement of micromechanical properties using random-fuzzy variables. *Review of Scientific Instruments*, 77(035107), 2006.

[24] M. Pertile and M. De Cecco. Uncertainty evaluation for complex propagation models by means of the theory of evidence. *MEASUREMENT SCIENCE AND TECHNOLOGY*, 19:1–10, 2008.

[25] Chin Wang Lou and Ming Chui Dong. A novel random fuzzy neural networks for tackling uncertainties of electric load forecasting. *Electrical Power and Energy Systems*, 73:34–44, 2015.

[26] Yan Tu, Xiaoyang Zhou, Jun Gang, Merrill Liechty, Jiuping Xu, and Benjamin Lev. Administrative and market-based allocation mechanism for regional water resources planning. *Resources, Conservation and Recycling*, 95:156?73, 2015.

[27] W. Jiang, A. Ferrero, S. Salicone, and Q. Zhang. An extension of kalman filter within the possibility theory. In *I2MTC 2017*, Turin, Italy, May 22-25, 2017.

[28] R. Faragher. A new approach to linear filtering and prediction problems. *IEEE Signal Processing Magazine*, pages 128–132, September 2012.

[29] R. Todling. Estimation theory and atmospheric data assimilation. In *Inverse Methods in Global Biogeochemical Cycles*, Geophysical Monograph Series. American Geophysical Union, Washington, D. C.:Wiley, 2000.

[30] Charles K. Chui and Guanrong Chen. *Kalman Filtering - with Real-Time Applications*. Springer Series in Information Sciences. Springer, iii edition, 2009.

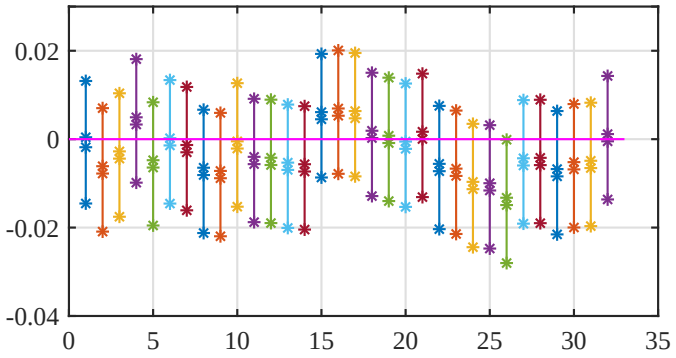

Fig. 10. Evolution of the α-cut widths at confidence level 0.95 for all 32 steps in the case shown in Fig. 9.

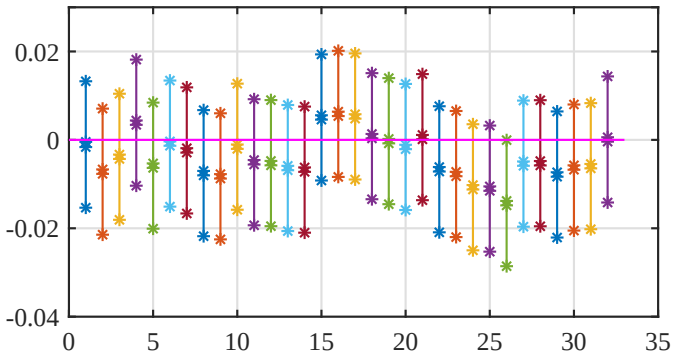

Fig. 11. Evolution of the α-cut widths at confidence level 0.95 for all 32 steps when the uncertainty contributions affecting the voltage supply are increased.

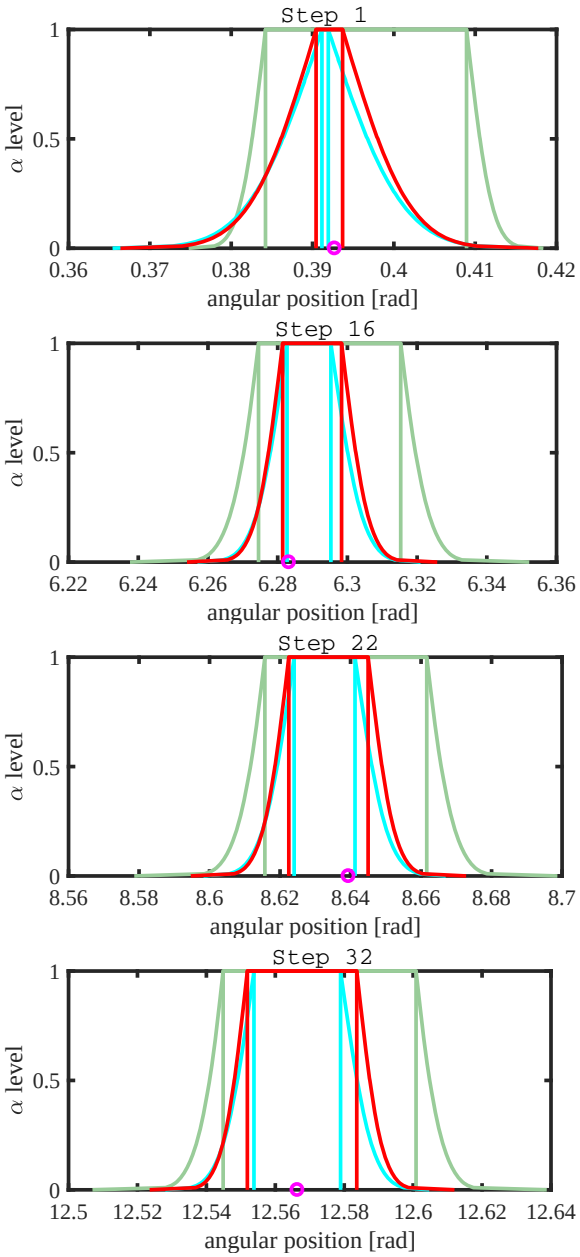

Fig. 12. Four step of the Kalman filters when random and systematic contributions are added to the voltage supply and the measured angular positions are affected by both random and systematic uncertainty contributions (CASE C). The green lines represent the obtained *a priori* RFVs (Θ_k^f), the cyan lines represent the RFVs associated to the measurements (Θ_k) and the red lines represents the obtained *a posteriori* RFVs (Θ_k^a). The pink circles represent the expected angular position.

[31] Erich Peter Klement, Radko Mesiar, and Endre Pap. Triangular norms. position paper I: basic analytical and algebraic properties. *Fuzzy Sets and Systems*, 143(1):5 – 26, 2004.

[32] A. Ferrero, M. Prioli, and S. Salicone. The construction of joint possibility distributions of random contributions to uncertainty. *IEEE Trans. Instrum. Meas.*, pages 1–9, 2013.

[33] A. Ferrero, M. Prioli, S. Salicone, and W. Jiang. Combination of measurement uncertainty contributions via the generalized dombi operator. In *Proceedings of the 2015 Conference of the International Fuzzy Systems Association and the European Society for Fuzzy Logic and Technology*, AISR, pages 1507–1513. Atlantis Press, 2015.

[34] A. Ferrero, M. Prioli, and S. Salicone. Processing dependent systematic contributions to measurement uncertainty. *IEEE Trans. Instrum. Meas.*, 4(62):1–12, 2013.

[35] D. Dubois, L. Foulloy, G. Mauris, and H. Prade. Probability-possibility transformations, triangular fuzzy sets, and probabilistic inequalities. *Reliable Computing. Kluwer Academic Publishers*, 10:273–297, 2004.

[36] A. Ferrero, M. Prioli, S. Salicone, and B. Vantaggi. 2D probability-possibility transformations. In *Synergies of Soft Computing and Statistics for Intelligent Data Analysis*, volume 190 of *Advances in Intelligent Systems and Computing*, pages 63–72. Springer Berlin Heidelberg, 2013.

[37] A. Ferrero, M. Prioli, and S. Salicone. Joint random-fuzzy variables: A tool for propagating uncertainty through nonlinear measurement functions. *IEEE Trans. Instrum. Meas.*, 65(5):1015–1021, May 2016.

[38] G. J. Klir and B. Yuan. *Fuzzy sets and fuzzy logic. Theory and applications*. Prentice Hall PTR, Englewood Cliffs, NJ, USA, 1995.

[39] A. Ferrero, M. Prioli, S. Salicone, and W. Jiang. Combination of measurement uncertainty contributions via the generalized dombi operator. In *16th World Congress of IFSA and 9th Conference of EUSFLAT*, pages 1507–1513, Gijón, Spain, June 30th ?July 3rd, 2015.

[40] C. Carlsson and R. Fullér. On possibilistic mean value and variance of fuzzy numbers. *Fuzzy sets and systems*, 122(2):315–326, September 2001.

[41] W. Jiang, A. Ferrero, S. Salicone, and Zhang Q. A possible way to perform recursive bayesian estimate in the possibility domain. *IEEE Trans. Instrum. Meas.*, 66(12):3218–3227, December 2017.

[42] A. Ferrero, M. Prioli, S. Salicone, and B. Vantaggi. A 2-D metrology-sound probability-possibility transformation. *IEEE Trans. Instrum. Meas.*, pages 1–9, 2013.

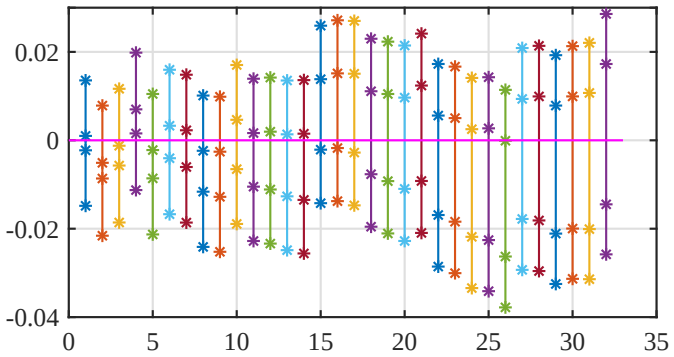

Fig. 13. Evolution of the α-cut widths at confidence level 0.95 for all 32 steps in the case shown in Fig. 12.